

## Article

# Deactivation of $V_2O_5-WO_3/TiO_2$ DeNO<sub>x</sub> Catalyst under Commercial Conditions in Power Production Plant

Maciej Zyrkowski <sup>1,2,\*</sup> , Monika Motak <sup>1</sup> , Bogdan Samojeden <sup>1,\*</sup>  and Krzysztof Szczepanek <sup>2</sup>

<sup>1</sup> Faculty of Energy and Fuels, AGH University of Science and Technology, al. Mickiewicza 30, 30-059 Kraków, Poland; motakm@agh.edu.pl

<sup>2</sup> PGE Energia Ciepła S.A., ul. Ciepłownicza 1, 31-587 Kraków, Poland; krzysztof.szczepanek@gkpge.pl

\* Correspondence: maciej.zyrkowski@agh.edu.pl (M.Z.); bogdan.samojeden@agh.edu.pl (B.S.)

Received: 2 November 2020; Accepted: 23 November 2020; Published: 25 November 2020



**Abstract:** Nitrogen dioxide is one of the most dangerous air pollutants, because its high concentration in air can be directly harmful to human health. It is also responsible for photochemical smog and acid rains. One of the most commonly used techniques to tackle this problem in large combustion plants is selective catalytic reduction (SCR). Commercial SCR installations are often equipped with a  $V_2O_5-WO_3/TiO_2$  catalyst. In power plants which utilize a solid fuel boiler, catalysts are exposed to unfavorable conditions. In the paper, factors responsible for deactivation of such a catalyst are comprehensively reviewed where different types of deactivation mechanism, like mechanical, chemical or thermal mechanisms, are separately described. The paper presents the impact of sulfur trioxide and ammonia slip on the catalyst deactivation as well as the problem of ammonium bisulfate formation. The latter is one of the crucial factors influencing the loss of catalytic activity. The majority of issues with fast catalyst deactivation occur when the catalyst work in off-design conditions, in particular in too high or too low temperatures.

**Keywords:** SCR-NH<sub>3</sub>; DeNO<sub>x</sub>; deactivation; power plants; vanadium-based catalyst; ammonium bisulfates; commercial catalyst

## 1. Introduction

Fossil fuel power plants are subjected to increasingly rigorous NO<sub>x</sub> emission limits. In Europe there are still plenty of coal-fired power generation units that produce significant amounts of nitrogen oxides. Two major types of NO<sub>x</sub> removal technology are used in such plants: selective non-catalytic reduction (SNCR) and selective catalytic reduction (SCR). As the name suggests, the latter takes advantage of a catalyst. The decision of choosing one over the other comes down to economic and technical aspects. While SNCR technology is much more affordable for power plant operators, it may struggle to deliver the required NO<sub>x</sub> emission reduction nowadays. The emission limits in current European Union (EU) regulations are 150 mg/Nm<sup>3</sup> for an existing large coal-fired boiler, 180 mg/Nm<sup>3</sup> for a medium-sized boiler and 270 mg/Nm<sup>3</sup> for small ones. For newly built units, limits are respectively 85, 100 and 150 mg/Nm<sup>3</sup> [1]. These limits favor utilization of SCR technology for medium and large existing units, as well as for all newly built ones.

Catalysts are a well-known technology in a variety of industries, and there is still a lot of ongoing research regarding the development of new catalysts and improvement of existing ones. Despite many advantages, catalysts tend to lose their activity over time. Kiełtyka et al. [2] indicated, that in a typical coal-fired power plant with biomass co-firing,  $V_2O_5-WO_3/TiO_2$  commercial catalyst can lose 10% of its

activity already after 2000 h of operation, and 20% after nearly 5000 h. According to Zheng et al. [3], the rate of deactivation of  $V_2O_5-WO_3/TiO_2$  catalyst installed on a straw-fired boiler can be as high as 1% per day of operation. Eventually catalytic layers need to be replaced every 2–3 years (in commercial installations), and new ones are relatively expensive [4,5].

Commercial catalysts installed on coal-fired boilers are subjected to rapidly changing and rather unfavorable conditions. The reactor is usually placed at the end of the boiler second pass (high-dust configuration). There are two main factors that are responsible for SCR catalyst deactivation—flue gas physical parameters and flue gas composition. The former is derived from various process parameters, boiler construction, as well as boiler load. The latter is derived mainly from fuel composition and the combustion process itself. The composition of flue gas is responsible for chemical deactivation of the catalyst (poisoning, plugging) as well as mechanical deactivation (erosion caused by coarse particles). Flue gas physical parameters are responsible for thermal deactivation (sintering due to the high temperature) and mechanical deactivation (uneven flue gases distribution) [5,6]. During the boiler operation, it is feasible to control both factors to a certain extent, depending on the boiler. One of the most commonly used catalysts in the power industry are vanadium-based catalysts, with 1 ÷ 2.5 wt.% of  $V_2O_5$  as an active material, 8 wt.% of  $WO_3$  as a promoter and anatase  $TiO_2$  as a supporter. They can be a plate-type or have the shape of a honeycomb [7]. Vanadium concentration is crucial for the  $NO_x$  reduction [8], however its high content may cause loss of the selectivity and thermal stability of the catalyst, as well as increased conversion of  $SO_2$  to  $SO_3$  [9–12]. The major drawback of  $V_2O_5-WO_3/TiO_2$  catalyst is its toxicity and the poor stability of vanadium, reduced activity at low temperature (below 250 °C) as well as a relatively narrow temperature window [10,13,14]. However, the catalyst is known for its high activity and resistance to  $SO_2$  [5,15–18]. According to literature,  $V_2O_5-WO_3/TiO_2$  catalysts work best in temperatures 300 ÷ 400 °C [19,20]. Operation at higher temperatures can cause sintering, while operation at lower temperatures may result in catalyst plugging due to ammonium bisulfate formation [21,22].

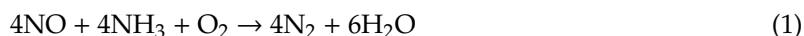
This paper gives detailed overview of the commercial  $V_2O_5-WO_3/TiO_2$  catalysts used in De $NO_x$  process in industrial boilers, with focus on the mechanisms of its deactivation. The mechanisms of  $SO_2$  oxidation, as well as ammonia slip from SCR reactors, are also described, as they are vital to understand the catalyst deactivation process. Furthermore, the authors describe the effect of boiler operation conditions on the overall catalyst performance.

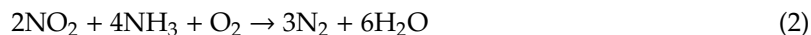
## 2. Catalyst Performance

Overall, an SCR catalyst's performance can be simply described by its ability to reduce concentration of  $NO_x$  from flue gas stream. This is a derivative of the catalyst's activity, which for heterogeneous catalysts can be approximated as the amount of active centers that the catalyst has. Active sites are regions of the solid catalyst, where free (unbalanced) chemical bonds exist allowing the adsorption process. In practice, active centers can be found in all distorted spots of the catalyst's surface, such as cracks, peaks and corners. The higher the surface area of the catalyst the more active centers it may comprise. Active centers can be also easily damaged by a variety of factors [23].

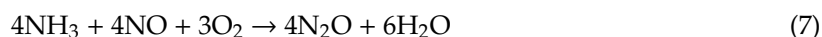
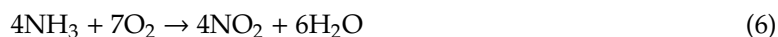
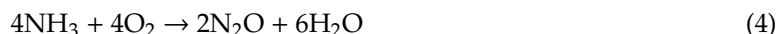
According to Odenbrand et al. and Li et al. catalyst deactivation is a mainly chemical phenomenon [24,25]. The role of active component in the catalyst is to provide sufficient amount of active sites. For the  $V_2O_5-WO_3/TiO_2$  catalyst, most important are V-OH acid sites and  $V^{5+} = O$  sites [15,26]. Vanadium oxide content is, therefore, responsible for catalyst activity, and its reduction during the SCR reactor's operation results in activity loss. For the  $V_2O_5-WO_3/TiO_2$  catalyst, the role of  $WO_3$  supporter is also considerable, as it interacts with  $TiO_2$  to enhance electron transfer as well as it helps with NO oxidation to  $NO_3^-$  and further decomposition of  $NO_3^-$  to  $NO_2$ . This is beneficial for catalyst activity and to widen the temperature window for the reaction [27,28].

The main reactions occurring in SCR installation in the presence of a catalyst, are:





Ammonia reduction over the  $\text{V}_2\text{O}_5\text{--WO}_3/\text{TiO}_2$  catalyst is highly selective, which means the NO is reduced before the  $\text{O}_2$ . Therefore reactions (1) and (2) proceed at the highest rate. Side reactions occurring in the SCR reactors are the following [29]:



Side reactions (4)–(7) are undesired, as they lead to formation of nitrogen oxides ( $\text{N}_2\text{O}$ , NO,  $\text{NO}_2$ ) instead of elementary nitrogen. Most often it is possible to detect some  $\text{N}_2\text{O}$  downstream the SCR reactor, and it is a strong greenhouse gas but it is hard to detect NO or  $\text{NO}_2$  in flue gas. However, increased consumption of reagent (particularly when SCR operating temperature exceeds  $380^\circ\text{C}$ ) can be an indication of their formation, according to Media et al. [29]. All the above equations indicate the key role of ammonia in the process [30]. To ensure the best performance of the SCR reactor, the proper  $\text{NH}_3/\text{NO}_x$  molar ratio is required. The highest  $\text{NO}_x$  reduction efficiency can be achieved for  $\text{NH}_3/\text{NO}_x$  molar ratio between 1.0 and 1.1. For a value of  $\text{NH}_3/\text{NO}_x$  higher than this, reduction efficiency remains constant but the ammonia slip strongly increases [31]. To start SCR reactions, ammonia must first be activated, which can occur either through Lewis-type interaction or over a Brønsted acidic site, of which the second mechanism is more favorable [32]. According to adsorption theory, a desired reaction is boosted by a catalyst wherever ammonia molecules (in Lewis-type interactions) or ammonia ions (in Brønsted acidic site) can adsorb on the surface [33,34]. Also the presence of sulfates increase Lewis and Brønsted acidity, which is beneficial for  $\text{NO}_x$  reduction capabilities as well as the catalyst lifetime [35,36]. Some authors refer to the catalyst storage capacity as the total amount of  $\text{NH}_3$  that can be adsorbed on the catalyst surface [37,38]. Another factor, important from the DeNO<sub>x</sub> reaction point of view, is a proper contact time between flue gas and the catalyst surface, therefore, too high a flue gas velocity can result in decreased  $\text{NO}_x$  removal efficiency [31].

Referring to the basics of the catalysis process, some more interesting facts can be derived. According to literature, the idea of the catalytic process is to reduce energy of activation required for a given reaction. Without the catalyst (i.e., in the SNCR method), the temperature in DeNO<sub>x</sub> reactions is equal to about  $950^\circ\text{C}$  [39,40]. For vanadium-based catalysts, maximum efficiency can be achieved in about  $350^\circ\text{C}$  [41]. However, NO conversion decreases from 100% at about  $270 \div 300^\circ\text{C}$  to only 20% at about  $120^\circ\text{C}$  [27]. According to Song et al. [42], who tested a  $\text{V}_2\text{O}_5\text{--MoO}_3/\text{TiO}_2$  catalyst, NO conversion can drop significantly also when temperature higher than  $350^\circ\text{C}$  is reached.

In pulverized coal boilers, it is difficult to maintain constant flue gas temperature and distribution. The temperature at which flue gas enters the reactor depends on multiple boiler parameters, such as for instance a coal mills configuration, the amount of air supplied to combustion and to over-fire nozzles, the cleanliness level of heating surfaces, the load of the boiler or feed water inlet temperature. Volatile matter content in coal can also influence flue gas temperature. If there are some regions of the SCR reactor that are exposed to lower flue gas flow, it may lead to faster deactivation of those regions due too. On the other hand, many of the above parameters can be controlled during the boiler operation, which gives room for optimization of SCR working conditions.

Because the catalyst's performance declines over time, it is important to measure its ability to reduce NO<sub>x</sub> from flue gas by means of an absolute factor. The performance of SCR catalysts, can be expressed as follows [23]:

$$X = 1 - \frac{C_{NO}^{out} + C_{NO_2}^{out}}{C_{NO}^{in} + C_{NO_2}^{in}} \quad (8)$$

$$V_{area} = \frac{V}{A} \quad (9)$$

$$K = -V_{area} \ln(1 - X) \quad (10)$$

where:

V<sub>area</sub>—area velocity [m<sup>3</sup>/m<sup>2</sup>h]

A—total surface area of the catalyst [m<sup>2</sup>]

V—flue gas volumetric flow through the catalyst [m<sup>3</sup>/h]

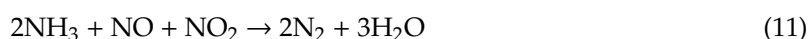
X, X<sub>0</sub>—efficiency of the catalyst (used, fresh)

C—concentration of inlet and outlet NO/NO<sub>2</sub>

K, K<sub>0</sub>—catalyst activity coefficient (used, fresh)

By dividing the activity coefficient K of an used catalyst by K<sub>0</sub> of a fresh catalyst, overall loss of activity can be calculated for the catalyst. As long as both the fresh and used catalysts are exposed to exactly the same volumetric flue gas flow and have exactly the same total surface area A (not the surface area measured by BET isotherm method), area velocity V<sub>area</sub> (Equations (9) and (10)) can be neglected. When a set of catalyst layers is under consideration, K values for each layer should be added to obtain the activity coefficient for a whole installation. Equation (10) can only be applied when NH<sub>3</sub>/NO<sub>x</sub> ratio is between 1.00 and 1.02, while Equation (8) can be used for a general assessment of the catalyst's performance [23].

Most desired improvements that are under research for vanadium-based catalyst are aimed to ensure its appropriate operation in the temperature range 200–250 °C [43]. According to Koebel et al. [44], rate of reaction at temperatures below 300 °C is limited by reoxidation of vanadium sites, which can be partially compensated by introducing NO<sub>2</sub>. However, almost all of NO<sub>x</sub> generated in combustion chamber is in the form of NO [45]. The way to improve a vanadium-based catalyst's performance at lower temperatures is to take advantage of the so-called "fast SCR" reaction. By increasing the fraction of NO<sub>2</sub> before the SCR reactor, which can be done by placing additional oxidation catalyst, the "fast SCR" reaction will occur [44,46]:



The activity of a vanadium-based catalyst at low temperature can be also improved by doping with elements, such as Co, Ce, Cr, Mo or Ni [47]. According to Li et al. [48], a small addition of silica to the TiO<sub>2</sub> supporter can improve catalyst selectivity towards N<sub>2</sub>. Activity of the vanadium-based catalyst can be increased by the addition of CeO<sub>2</sub>, done by the impregnation or co-precipitation methods. This allows us to increase activity of the catalyst, widen the temperature window of the reaction, as well as improve resistance to sulfur [49,50].

### 3. Problem of Ammonia Bisulfate Formation

#### 3.1. Ammonia Slip

In order to abate NO<sub>x</sub> emission by employing selective-catalytic reduction methods, the flue gas from a power plant is mixed with liquid ammonia (NH<sub>3</sub>) in the presence of catalyst. Ammonia is injected to the flue gas stream at the inlet of the SCR reactor by means of spray nozzles. Typically, not all of the injected ammonia reacts and a part of it is carried over by the flue gas stream and escapes

the SCR reactor. This amount of  $\text{NH}_3$  is usually called the ammonia slip [51,52]. As already mentioned, ammonia slip appears when  $\text{NH}_3/\text{NO}_x$  ratio is higher than 1 [31]. There are several reasons why this phenomenon is highly undesired from the power plant operation point of view. Escaped ammonia would react with  $\text{SO}_3$  in flue gas, creating sticky ammonium bisulfates that can easily collect dust and plug not only SCR catalysts, but also devices such as rotating air preheaters. Besides the formation of sulfates, ammonia can also adsorb on the fly ash. In particular, adsorption occurs when there is amorphous structure in fly ash particles. Therefore, it is also linked with the combustion process and boiler load, as faster flue gas cooling leads to the presence of amorphous phase in the particles [53–58]. Escaped ammonia may thus affect the quality of fly ash from the power plant—the material that is typically sold on the market. A strong smell of ammonia may hinder fly ash from being utilized, which would generate additional costs for the power plant. It is worth mentioning that total ammonia adsorbed by fly ash depends not only on the level of ammonia slip from SCR reactors, but also on the fly ash structure and composition. An acceptable value of ammonia slip from SCR reactor is in the range of 1–2 ppmv while slip higher than 5 ppmv should be avoided [59]. A typical reason for ammonia slip that is too large are poor ammonia distribution in flue gas, catalyst age and contamination, low flue gas temperature, inlet  $\text{NO}_x$  level higher than SCR reactor design point as well high flue gas flow.

### 3.2. Sulfur Trioxide

One of the crucial factors for both boiler and SCR catalysts' operation is the concentration of sulfur trioxide ( $\text{SO}_3$ ). Its presence in the flue gas stream is derived from the  $\text{SO}_2$  to  $\text{SO}_3$  conversion. There are several factors determining this phenomenon. The most important is sulfur content in coal which is mostly converted to  $\text{SO}_2$  in the combustion chamber. Another is oxygen concentration—the more oxygen present in the combustion process, the higher the  $\text{SO}_3$  concentrations will be [60]. Most of the  $\text{SO}_3$  formation in the combustion chamber takes place at temperatures above 530 °C. A high content of alkaline/earth-alkaline compounds (CaO in particular) would result in lower  $\text{SO}_3$  concentration, due to formation of sulfates. These reactions are most likely to happen in the temperature range 300–800 °C. The  $\text{SO}_2/\text{SO}_3$  conversion is, on the other hand, catalyzed by the presence of iron oxide ( $\text{Fe}_2\text{O}_3$ ) in flue gas. This catalytic conversion is most intense at about 600–700 °C (it does vary depending on the  $\text{Fe}_2\text{O}_3$  particle size) and it has the most significant effect on the final  $\text{SO}_3$  concentration in flue gas [60]. Also the presence of alumina, CuO and  $\text{V}_2\text{O}_5$  results in a higher  $\text{SO}_2/\text{SO}_3$  conversion rate. Typical conversion upstream of the SCR reactor in a pulverized coal boiler is within the range of 1–2% [55,61–64]. In a coal-fired boiler, all the aforementioned parameters are subjected to dynamic changes. Therefore,  $\text{SO}_3$  concentration at the outlet of the combustion chamber may vary significantly and cannot be robustly predicted without a dedicated measurement system [65].

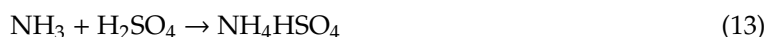
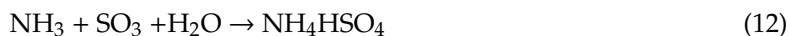
Downstream of the combustion chamber, the concentration of  $\text{SO}_3$  in a flue gas further increases when passing the SCR reactor. Next to the ammonia slip, high  $\text{SO}_2/\text{SO}_3$  conversion is another undesired parameter of the SCR installations. Depending on the catalyst wear and operating conditions,  $\text{SO}_2/\text{SO}_3$  conversion rate can reach up to 2% for the  $\text{V}_2\text{O}_5\text{-WO}_3/\text{TiO}_2$  catalyst. The conversion rate increases with temperature—at the temperature of 400 °C it can be more than twice the value obtained at 300 °C. Also, the  $\text{SO}_2/\text{SO}_3$  conversion increases proportionally to  $\text{NH}_3$  concentration. According to Lu et al. [66], conversion can increase from 1.1% to 2.1% when  $\text{NH}_3$  concentration increases from 40 ppm to 140 ppm. Furthermore, the content of  $\text{TiO}_2$  and  $\text{V}_2\text{O}_5$  can significantly affect the conversion. On the other hand, the  $\text{SO}_2/\text{SO}_3$  conversion in a SCR reactor increases by roughly 30% in the absence of ammonia injection. This occurs because the lack of  $\text{NH}_3$  makes the catalyst pores more accessible for  $\text{SO}_2$  adsorption and, therefore, contact with  $\text{TiO}_2$  and  $\text{V}_2\text{O}_5$  is increased [55,63,66–68]. According to the results published by Electric Power Research Institute [69],  $\text{SO}_2/\text{SO}_3$  conversion rate increases also with catalyst age as well as for the regenerated catalysts. The effect of  $\text{H}_2\text{O}$  on the  $\text{SO}_2/\text{SO}_3$  conversion is not consistent. According to Qing et al. [70], a rise in conversion can be visible for  $\text{H}_2\text{O}$  concentration in a flue gas between 7.5% and 15%, while for higher concentrations a visible drop can be noticed.



Sulfur trioxide is responsible for the formation of sulfuric acid in a flue gas from coal-fired power plants and it participates in ammonium bisulfate formation. The pure form of  $\text{SO}_3$  gas exists at the temperature higher than  $427^\circ\text{C}$ . As the temperature drops along the boiler path,  $\text{SO}_3$  combines with water vapor forming  $\text{H}_2\text{SO}_4$ . This process ends when temperature reaches about  $200^\circ\text{C}$ , when almost all  $\text{SO}_3$ —that has not reacted with ammonia in the meantime—is converted to sulfuric acid [67,71]. The latter may condense at temperature below ca.  $200^\circ\text{C}$  [72], which can lead to serious corrosion issues [71].

### 3.3. Ammonia Bisulfate Formation

Both ammonia slip and sulfur trioxide influence the formation of ammonium bisulfates (ABS), sticky and corrosive substances that block active sites on the catalyst [17,42,73,74]. According to Wang et al. [75], the deposition of 30% wt.  $\text{NH}_4\text{HSO}_4$  on the catalyst results in a pore volume drop of more than 50% and a significant reduction in BET surface area. When ABS starts depositing, firstly the larger pores are affected and smaller pores remain untouched. If the temperature of flue gas is above the ABS dew point, condensation can still occur inside the catalyst pores. Crucial chemical reactions that describe ABS formation in a coal-fired boiler are [76]:



The obvious way to abate issues with ABS is to avoid or decrease its formation. The latter is proportional to the concentration of  $\text{SO}_3$ , moisture and  $\text{H}_2\text{SO}_4$  in the flue gas, as well as ammonia slip from SCR reactors. The latter increases when the catalyst activity drops, which indicates the relation between ammonia slip and other mechanisms of deactivation, such as a decrease in Brønsted acid sites for instance. The higher the concentration of  $\text{NH}_3$ ,  $\text{SO}_3$  and moisture in flue gas, the higher the temperature of ABS condensation [76,77]. It is important to determine the accurate temperature of ABS condensation, because the temperature of flue gas varies significantly with the boiler load [61]. Knowing the edge temperature allows to operate the boiler in a manner that could prevent ABS condensation. However, there is no consistency in the literature about the temperature of ABS condensation. Furthermore, the temperature of  $\text{NH}_4\text{HSO}_4$  decomposition on the catalyst surface can be higher due to the specific pore structure. If catalyst pore size decreases below 10 nm, the decomposition temperature increases due to the capillary forces [55,65]. According to Menasha et. al. [77], ABS can precipitate in the temperature range of  $262\text{--}327^\circ\text{C}$ , with peak intensity in the range of  $284\text{--}300^\circ\text{C}$ . Shi et al. [78] pointed out that the temperature of ABS condensation is in the range of  $190\text{--}240^\circ\text{C}$ . It can be concluded that at the temperature below ca.  $330^\circ\text{C}$ , there is a risk of ammonia bisulfate precipitation. Producers, knowing the actual pore structure, can define the minimum safe operating temperature for a catalyst, such as presented in Figure 1 [65]. Power plant operators may consider closing  $\text{NH}_3$  injection if the actual temperature of the flue gas is lower than the minimum safe temperature, as operating the SCR reactor below the ABS dew point can be seriously damaging for catalyst activity. Results of laboratory tests show that after 20 h of operation in such conditions, coefficient  $K/K_0$  is equal to ca. 0.6 for the first layer and 0.8 for the second layer of the SCR reactor [76,77]. Ammonium bisulfates is also dangerous for devices placed downstream the SCR reactor. In a coal-fired power plant, the rotating air preheater is typically affected due to increased fouling, which is a highly undesirable phenomenon [79].

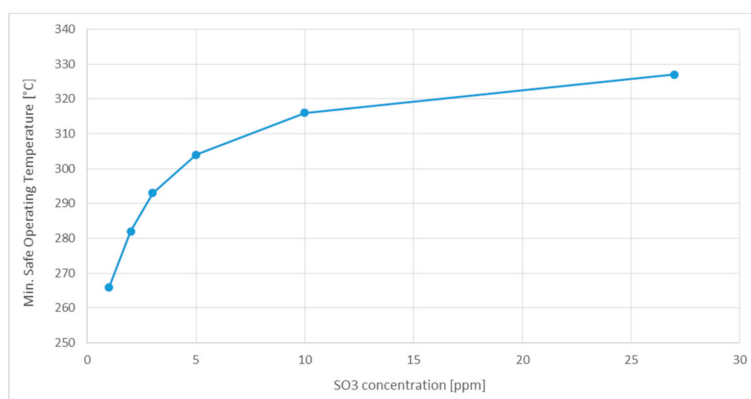


**Figure 1.** Minimum safe operating temperature for selective catalytic reduction (SCR) reactors as the function of SO<sub>3</sub> concentration, according to Charles [65].

#### 4. Deactivation Mechanisms

Catalyst deactivation phenomena can be divided into three major types—mechanical, chemical and thermal deactivation [6]. As far as chemical deactivation is concerned, it is vital to discuss issues related with catalyst poisoning which, besides already discussed ammonium bisulfates formation, are crucial for the V<sub>2</sub>O<sub>5</sub>–WO<sub>3</sub>/TiO<sub>2</sub> catalyst operation.

##### 4.1. Poisoning

Poisoning of the SCR catalyst is mainly associated with alkali metals and sulfur. Also, water present in the flue gas can affect activity of the vanadium-based catalyst as it occupies acidic sites [80]. The concentration of water vapor equal to 8% in a flue gas can decrease activity by roughly 15% after 3 h of operation. If water is removed from the flue gas, however, activity is restored to the initial level [41]. At temperature above 450 °C, however, moisture can enhance NO<sub>x</sub> conversion [81]. The V<sub>2</sub>O<sub>5</sub>–WO<sub>3</sub>/TiO<sub>2</sub> catalyst is well known for its resistance to SO<sub>2</sub> poisoning. Despite that, such catalysts are still affected by sulfur dioxide content in the flue gas, particularly when the flue gas temperature drops below 300 °C [82]. Its presence allows compounds to form that are directly responsible for catalyst deactivation or plugging. The role of pure SO<sub>2</sub> is also significant. According to Zang et al. [83], SO<sub>2</sub> adsorption on the catalyst occurs and SO<sub>4</sub><sup>2−</sup> ions are formed as the result, particularly in the presence of oxygen, and they can occupy active sites of the catalyst. Xiao et al. [84] indicated, that when adding roughly 1000 ppm of pure SO<sub>2</sub> to the flue gas stream, the activity of the catalyst can drop by ca. 20%. The major reason for V<sub>2</sub>O<sub>5</sub>–WO<sub>3</sub>/TiO<sub>2</sub> catalyst deactivation is, however, related to interactions with alkali metals present in flue gas. As the temperature required by the V<sub>2</sub>O<sub>5</sub>–WO<sub>3</sub>/TiO<sub>2</sub> catalyst is relatively high, the most common position of the SCR installation is upstream of the dust collector (called a high-dust SCR) [2,6,85]. Because of that, the catalyst surface interacts with alkali and earth alkali metals carried out by the flue gas stream. Along with the SO<sub>2</sub>, alkali metals can poison the catalyst and, in consequence, reduce its activity. One of the major reasons for that is the neutralization of acid sites. Sodium, calcium and potassium are known to have the most damaging effect on the vanadium-based catalysts [86–91]. Tang et al. [92] confirmed that cations Na<sup>+</sup> and Ca<sup>2+</sup> can affect the activity of the catalyst, due to neutralization of Brønsted acid sites as well as a decrease of vanadium reducibility. The CaSO<sub>4</sub>, responsible for plugging the catalyst as well as increased emission of N<sub>2</sub>O, is formed when Ca combines with SO<sub>2</sub> and O<sub>2</sub> [89,93–95]. Also the CaO and CaCO<sub>3</sub> reduce catalyst activity [95]. Deng et al. studied the effect of NaCl, KCl, Na<sub>2</sub>CO<sub>3</sub>, K<sub>2</sub>CO<sub>3</sub>, Na<sub>2</sub>SO<sub>4</sub> and K<sub>2</sub>SO<sub>4</sub> on the catalyst's performance. In the worst case scenario, the V<sub>2</sub>O<sub>5</sub>–WO<sub>3</sub>/TiO<sub>2</sub> catalyst exposed to the stream of pure KCl and NaCl aerosol for 5 h lost, respectively, about 26% and 16% of its initial efficiency. At low K/V molar ratios (range 0.02–0.1), K<sub>2</sub>S<sub>2</sub>O<sub>7</sub> is formed and it interacts with V<sub>2</sub>O<sub>5</sub>. The product of this interaction—eutectic V<sub>2</sub>O<sub>5</sub>–K<sub>2</sub>S<sub>2</sub>O<sub>7</sub>—decreases NH<sub>3</sub> adsorption on Brønsted acid

sites [25]. Zheng et al. [95] tested deactivation of a catalyst exposed to a pure KCl and K<sub>2</sub>SO<sub>4</sub> stream and concluded that the main reason for deactivation was reaction between poison and Brønsted acid sites. The compounds, such as Na<sub>2</sub>CO<sub>3</sub>, K<sub>2</sub>CO<sub>3</sub>, Na<sub>2</sub>SO<sub>4</sub> or K<sub>2</sub>SO<sub>4</sub>, as well as the presence of KCl and NaCl in coal, results in lower, but still clearly noticeable deactivation [6,87]. According to Xiao et al. [84], Na<sub>2</sub>O can decrease the number of V<sup>5+</sup> = O bonds as well as the surface oxygen, which affect NO<sub>x</sub> conversion. Li et al. [41] compared the loss of V<sub>2</sub>O<sub>5</sub>–WO<sub>3</sub>/TiO<sub>2</sub> catalyst activity due to poisoning by different alkali metals. Tests revealed that the most damaging effect on the catalyst was from NaOH, followed by Na<sub>2</sub>O, Al(OH)<sub>3</sub> and Al<sub>2</sub>O<sub>3</sub>. Already 0.5% concentration of NaOH in flue gas is sufficient to decrease catalyst activity by 20% at 400 °C temperature and almost 40% at 350 °C. The presence of SO<sub>2</sub>, despite its negative effect in other situations, can abate deactivation caused by K, Na and Ca [2,96]. On top of that, Guo et al. [32] suggested, despite the negative effect of CaSO<sub>4</sub>, that sulfation can be actually beneficial for the catalyst activity as it increases the number of active Brønsted acid sites. According to Liu et al., the presence of Cl in flue gas can inhibit adsorption of NH<sub>3</sub> and NO<sub>x</sub> on the catalyst, which would affect its activity as well [90,97]. Another element that is capable of decreasing catalyst activity is phosphorus [30,98]. Also, arsenic has been reported as a poisonous element for vanadium-based catalyst which, along with the toxicity of vanadium, is the reason why spent catalysts are treated as a hazardous waste [5,99,100].

#### 4.2. Mechanical Deactivation

In coal-fired boilers, flue gas entering the SCR reactors contains a significant amount of particulate matter, such as fly ash particles, cenospheres or unburnt coal particles [57]. They hit the surface of catalysts at some point with a given momentum and can damage the surface, cause surface attrition or result in dust build-up in some areas of the SCR reactors [101]. Mechanical damage of the catalyst's surface, dust accumulation as well as attrition will result in the decrease of activity, affecting the number of available active sites. In an ideal situation, flow through the catalyst's plates should be optimized in such a way that the interaction between flue gas and SCR reactor surface has minimal impact on the catalyst's performance. Besides that, the amount of ammonia injected per unit of flue gas volume should be uniform. In industrial reality, flue gas distribution and velocity are usually uneven, which can affect a catalyst's performance [101–103]. In order to ensure a uniform distribution of flue gas entering the SCR reactor, installations are typically equipped with guide vanes directing the flow [104]. This solution might not be sufficient, however, as the flue gas distribution can pivot between left and right side of the boiler during its operation, so theoretically vanes should be able to dynamically adjust to the inlet flue gas distribution.

#### 4.3. Thermal Deactivation

Thermal deactivation of the catalyst is related to TiO<sub>2</sub> phase transition (or sintering). The TiO<sub>2</sub> most commonly occurs as one of two polymorphs—rutile or anatase. The rutile form is stable, while the anatase is stable only below certain temperature and can undergo irreversible phase transition to rutile. This process is influenced by the temperature at first place, but also particle size and shape, surface area, excess of oxygen or presence of promoters and inhibitors. Temperature of the transition can vary from 400 °C to 1200 °C, although it is mostly expected at roughly 600–750 °C. Elements, such as K, Na, Ni, Li, Fe, Zn, Cu, Cd, Mn and Cr, may act as promoters while elements, such as Ca, Si, P, S, Zr, Al, Ba, B and Ce may act as inhibitors [105–109]. Du et al. [110] pointed out that if the structure of TiO<sub>2</sub> is hollow, it could be possible to avoid phase transition at temperatures below 800 °C. Also, an amorphous carbon coating can prevent transition, by hindering the access of oxygen. One of the roles of tungsten in the V<sub>2</sub>O<sub>5</sub>–WO<sub>3</sub>/TiO<sub>2</sub> catalyst is to reduce phase transition of TiO<sub>2</sub> at high temperature [111,112]. However, according to Khutan et al. [113], temperature of the transition can be decreased by vanadium doping, which might be unfavorable for SCR catalysts containing both anatase TiO<sub>2</sub> and V<sub>2</sub>O<sub>5</sub>.

Thermal deactivation can result in overall surface area decrease and changes in surface structure resulting in a larger share of NH<sub>3</sub> adsorbed on Lewis-type sites. High temperature can also provoke



vanadium volatilization [14,114–116]. As a result, the activity of the catalyst is affected as well as the temperature window for DeNO<sub>x</sub> reaction becoming narrower. Besides that, the SO<sub>2</sub>/SO<sub>3</sub> conversion increases, which can make the catalyst eventually unusable [117].

## 5. Industrial Boilers Characteristics

SCR reactors equipped with a V<sub>2</sub>O<sub>5</sub>-WO<sub>3</sub>/TiO<sub>2</sub> catalyst are widely used in the power production sector. A pulverized coal boiler is a good example of SCR application unit with its rather difficult and rapidly changing operation conditions. According to Ma et al. [118], NO<sub>x</sub> specific emission from coal-fired units is lower for high capacity units, as well as for units burning bituminous coal. In typical configuration, the standard SCR reactor is placed at the end of the boiler, upstream of the air preheater. It must be designed specifically for each unit in order to locate reactors in the best temperature conditions. There are plenty of issues related to such configuration.

In the coal-fired power plant, temperature variation is a common problem. In the combustion chamber temperature can be as high as 1700–1900 °C and it decreases along the flue gas path [57]. The SCR reactors are typically installed close to the boiler outlet or the economizer (water heater). The temperature of flue gas entering the reactor depends on a variety of factors. The first is the combustion process itself, where the temperature depends mainly on the amount of air (oxygen) in the process as well as volatile matter content in coal [119]. The temperature of flue gas leaving the combustion chamber will depend on the firing system configuration and whether there is air staging or auxiliary air supply. Afterwards, flue gases are cooled down by means of heat exchangers (superheaters, economizers) along their pathway. If heating surfaces in the boiler are contaminated, temperature of the flue gas downstream of a given heat exchanger will be higher due to reduced heat transfer. Temperature in the combustion chamber may also fluctuate rapidly due to the difference in fuel properties, as coal fed to the boiler does not have a consistent composition most of the time. Any temperature fluctuation in the combustion chamber is going to propagate and probably affect the temperature of flue gas before the SCR reactors. Another factor that may influence this parameter is steam—its flow and temperature in the boiler, as well as cooling water injection level. Finally, the load changes. Depending on the boiler construction, the load level can decrease to about 40%. In older constructions equipped with a drum, this is usually 60%. The decreased load also results in lower flue gas temperature entering the SCR reactor [61]. Figure 2 presents a correlation between flue gas temperature, measured in the second pass of the boiler, and the load level for a medium-size, 120 kg/s nominal steam capacity, pulverized coal-fired boiler (hard coal). As can be seen, maximum flue gas temperature variation is equal to about 41 °C. Taking this into account, it can be concluded that the operation of the SCR reactor within optimal temperature range in coal-fired boilers can be difficult to achieve.

Moreover, in coal-fired boilers it is not easy to maintain an even flue gas distribution in the cross-section of the duct. It is a common knowledge that most of the time, the parameters of the flue gas in the boiler are offset to the right or left side, and hardly ever are they distributed evenly. This depends on the burners' configuration (tangential or front wall), as well as appropriate pulverized coal and air distribution in each of the burner and auxiliary air nozzles. The flue gas distribution can also depend on the cleanliness of the boiler heating surfaces. For instance, an intense dust built up on the one side of superheater causes additional pressure drop and thus disturbs the flue gas distribution downstream of this superheater [120]. It is also difficult to control the flue gas distribution during boiler operation and it is often impossible to obtain real-time information about this distribution. Some estimations can be made, however, by taking into account the temperature measurement along the boiler or ID fans' power consumption. CFD (Computational Fluid Dynamics) modelling is often employed to get knowledge about the real flue gas distribution, but it would be rather difficult to have such model working on-line in the power plant (although technically possible).

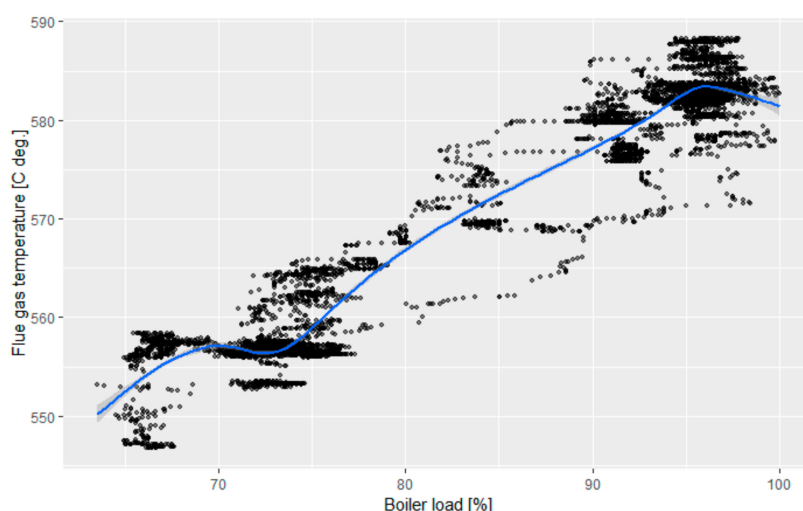


**Figure 2.** Correlation between flue gas temperature and the load level of pulverized-coal boiler with 120 kg/s nominal steam capacity (own source).

## 6. Conclusions

In the article, deactivation factors of vanadium-based catalyst for the DeNO<sub>x</sub> process have been comprehensively reviewed. They can be divided into three major categories: chemical, mechanical and thermal deactivation. As suggested by literature, the main problems influencing the operation of SCR reactors are the formation of SO<sub>3</sub> and ammonia slip. Both have a crucial effect on the formation of ammonium bisulfates, which is one of the most undesired side-products of DeNO<sub>x</sub> processes in coal-fired power plants. Ammonia bisulfate is a sticky substance, capable of clogging the surface of the catalyst as well as other equipment downstream of the SCR reactor. It is also responsible for a vast share of chemical deactivation of the catalyst, next to the poisoning arising from the presence of alkali and earth alkali metals in flue gas. The role of sulfur is ambiguous. On the one hand, it contributes to the ammonia bisulfate formation, but on the other hand, sulfation can increase the number of active Brønsted acid sites which is beneficial for catalyst activity. The latter can be also decreased by operating the SCR reactor at too high or low temperatures. Above 400 °C there is a risk of TiO<sub>2</sub> phase transition, while below 300 °C activity drops due to reaction kinetics as well as the effect of sulfur, alkali metals and ammonium bisulfates. A commercial SCR reactor installed on a pulverized coal boiler, is subjected to rapid and vast flue gas temperature fluctuations. Also, uneven flue gas distribution can result in a significant temperature difference along the reactor cross-section. Besides that, uneven flue gas distribution is responsible for faster deactivation of some parts of the catalysts due to attrition or dust build-up.

**Author Contributions:** Conceptualization, M.M. and B.S.; methodology, M.Z.; formal analysis, M.Z.; investigation, M.Z.; resources, M.Z.; data curation, M.Z.; writing—original draft preparation, M.Z. and B.S.; writing—review and editing, B.S. and K.S.; visualization, M.Z.; supervision, M.M. and K.S.; project administration, M.M.; funding acquisition, M.M. All authors have read and agreed to the published version of the manuscript.

**Funding:** This research was founded by the grant of the Ministry of Science and Higher Education no. 0039/DW/2018/02.

**Conflicts of Interest:** The authors declare no conflict of interest.

## References

1. UE. “Directive Implementation UE 2017/1442 from 31st of July 2017,” [Online]. Available online: [http://data.europa.eu/eli/dec\\_impl/2017/1442/oj](http://data.europa.eu/eli/dec_impl/2017/1442/oj). (accessed on 23 September 2020).
2. Kiełtyka, M.; Dias, A.P.S.; Kubiczek, H.; Sarapata, B.; Grzybek, T. The influence of poisoning on the deactivation of DeNO<sub>x</sub> catalysts. *C. R. Chim.* **2015**, *18*, 1036–1048. [CrossRef]

3. Zheng, Y.; Jensen, A.D.; Johnsson, J.E. Deactivation of  $V_2O_5$ - $WO_3$ - $TiO_2$  SCR catalyst at a biomass-fired combined heat and power plant. *Appl. Catal. B Environ.* **2005**, *60*, 253–264. [\[CrossRef\]](#)
4. Yu, Y.; Chi, H.E.; Chen, J.; Meng, X. Deactivation mechanism of de- $NO_x$  catalyst ( $V_2O_5$ - $WO_3$ / $TiO_2$ ) used in coal fired power plant. *J. Fuel Chem. Technol.* **2012**, *40*, 1359–1365. [\[CrossRef\]](#)
5. Li, M.; Liu, B.; Wang, X.; Yu, X.; Zheng, S.; Du, H.; Dreisinger, D.; Zhang, Y. A promising approach to recover a spent SCR catalyst: Deactivation by arsenic and alkaline metals and catalyst regeneration. *Chem. Eng. J.* **2018**, *342*, 1–8. [\[CrossRef\]](#)
6. Deng, L.; Liu, X.; Cao, P.; Zhao, Y.; Du, Y.; Wang, C.; Che, D. A study on deactivation of  $V_2O_5eWO_3eTiO_2$  SCR catalyst by alkali metals during entrained-flow combustion. *J. Energy Inst.* **2017**, *90*, 743–751. [\[CrossRef\]](#)
7. Tomasic, V. Application of the monoliths in De $NO_x$  catalysis. *Catal. Today* **2007**, *119*, 106–113. [\[CrossRef\]](#)
8. Soleimanzadeh, H.; Niaei, A.; Salari, D.; Tarjomannejad, A.; Penner, S.; Grunbacher, M.; Hosseini, S.A.; Mousavi, S.M. Modeling and optimization of  $V_2O_5/TiO_2$  nanocatalysts for  $NH_3$ -Selective catalytic reduction (SCR) of  $NO_x$  by RSM and ANN techniques. *J. Environ. Manag.* **2019**, *238*, 360–367. [\[CrossRef\]](#)
9. Rauch, D.; Albrecht, G.; Kubinski, D.; Moos, R. A microwave-based method to monitor the ammonia loading of a vanadia-based SCR catalyst. *Appl. Catal. B Environ.* **2015**, *165*, 36–42. [\[CrossRef\]](#)
10. Song, I.; Youn, S.; Lee, H.; Lee, S.G.; Cho, S.J.; Kim, D.H. Effects of microporous  $TiO_2$  support on the catalytic and structural properties of  $V_2O_5$ /microporous  $TiO_2$  for the selective catalytic reduction of  $NO$  by  $NH_3$ . *Appl. Catal. B Environ.* **2017**, *210*, 421–431. [\[CrossRef\]](#)
11. He, Y.; Ford, M.E.; Zhu, M.; Liu, Q.; Tumuluri, U.; Wu, Z.; Wachs, I.E. Influence of catalyst synthesis method on selective catalytic reduction (SCR) of  $NO$  by  $NH_3$  with  $V_2O_5$ - $WO_3$ / $TiO_2$  catalysts. *Appl. Catal. B Environ.* **2016**, *193*, 141–150. [\[CrossRef\]](#)
12. Yates, M.; Martin, J.A.; Martin-Luengo, M.A.; Suarez, S.; Blanco, J.  $N_2O$  formation in the ammonia oxidation and in the SCR process with  $V_2O_5$ - $WO_3$  catalysts. *Catal. Today* **2005**, *107*, 120–125. [\[CrossRef\]](#)
13. Huang, Y.; Tong, Z.; Wu, B.; Zhang, J. Low temperature selective catalytic reduction of  $NO$  by ammonia over  $VxO_5$ - $CeO_2$ / $TiO_2$ . *J. Fuel Chem. Technol.* **2008**, *36*, 616–620. [\[CrossRef\]](#)
14. Zhou, X.; Huang, X.; Xie, A.; Lou, S.; Yao, C.; Li, X.; Zuo, S.  $V_2O_5$ -decorated Mn-Fe/attapulgite catalyst with high  $SO_2$  tolerance for SCR of  $NO_x$  with  $NH_3$  at low temperature. *Chem. Eng. J.* **2017**, *326*, 1074–1085. [\[CrossRef\]](#)
15. Nicosia, D.; Czekaj, I.; Krocher, O. Chemical deactivation of  $V_2O_5$ / $WO_3$ - $TiO_2$  SCR catalysts by additives and impurities from fuels, lubrication oils and urea solution Part II. Characterization study of the effect of alkali and alkaline earth metals. *Appl. Catal. B Environ.* **2008**, *77*, 228–236. [\[CrossRef\]](#)
16. Wan, Q.; Duan, L.; Li, J.; Chen, L.; He, K.; Hao, J. Deactivation performance and mechanism of alkali (earth) metals on  $V_2O_5$ - $WO_3$ / $TiO_2$  catalyst for oxidation of gaseous elemental mercury in simulated coal-fired flue gas. *Catal. Today* **2011**, *175*, 189–195. [\[CrossRef\]](#)
17. Youn, S.; Song, I.; Lee, H.; Cho, S.J.; Kim, D.H. Effect of pore structure of  $TiO_2$  on the  $SO_2$  poisoning over  $V_2O_5$ / $TiO_2$  catalysts for selective catalytic reduction of  $NO_x$  with  $NH_3$ . *Catal. Today* **2018**, *303*, 19–24. [\[CrossRef\]](#)
18. Hammershoi, P.S.; Jangjou, Y.; Epling, W.S.; Jensen, A.D.; Janssens, T.V. Reversible and irreversible deactivation of Cu-CHA  $NH_3$ -SCR catalysts by  $SO_2$  and  $SO_3$ . *Appl. Catal. B Environ.* **2018**, *226*, 38–45. [\[CrossRef\]](#)
19. Bai, S.; Wang, Z.; Li, H.; Xu, X.; Liu, M.  $SO_2$  promotion in  $NH_3$ -SCR reaction over  $V_2O_5$ /SiC catalyst at low temperature. *Fuel* **2017**, *194*, 36–41. [\[CrossRef\]](#)
20. Samojeden, B.; Grzybek, T. The influence of the promotion of N-modified activated carbon with iron on  $NO$  removal by  $NH_3$ -SCR (Selective catalytic reduction). *Energy* **2016**, *116*, 1484–1491. [\[CrossRef\]](#)
21. Zhang, P.; Chen, T.; Zou, X.; Zhu, C.; Chen, C.; Liu, H.  $V_2O_5$ /hematite catalyst for low temperature selective catalytic reduction of  $NO_x$  with  $NH_3$ . *Chin. J. Catal.* **2014**, *35*, 99–107. [\[CrossRef\]](#)
22. Kowalczyk, A.; Świąt, A.; Gil, B.; Rutkowska, M.; Piwowarska, Z.; Borch, A.; Michalik, M.; Chmielarz, L. Effective catalysts for the low-temperature  $NH_3$ -SCR process based on MCM-41 modified with copper by template ion-exchange (TIE) method. *Appl. Catal. B Environ.* **2018**, *237*, 927–937. [\[CrossRef\]](#)
23. EPRI. *Laboratory Testing Protocol for Coal-Fired SCR Catalyst*, 3rd ed.; Report no. 3002013048; Electric Power Research Institute: Palo Alto, CA, USA, 2018.
24. Odenbrand, C.  $CaSO_4$  deactivated  $V_2O_5$ - $WO_3$ / $TiO_2$  SCR catalyst for a diesel power plant. Characterization and simulation of the kinetics of the SCR reaction. *Appl. Catal. B Environ.* **2018**, *234*, 365–377. [\[CrossRef\]](#)

25. Li, Q.; Chen, S.; Liu, Z.; Liu, Q. Combined effect of KCl and SO<sub>2</sub> on the selective catalytic reduction of NO by NH<sub>3</sub> over V<sub>2</sub>O<sub>5</sub>/TiO<sub>2</sub> catalyst. *Appl. Catal. B Environ.* **2015**, *164*, 475–482. [CrossRef]
26. Wang, J.; Miao, J.; Yu, W.; Chen, Y.; Chen, J. Study on the local difference of monolithic honeycomb V<sub>2</sub>O<sub>5</sub>-WO<sub>3</sub>/TiO<sub>2</sub> denitration catalyst. *Mater. Chem. Phys.* **2017**, *198*, 193–199. [CrossRef]
27. Zhang, S.; Zhong, Q. Surface characterization studies on the interaction of V<sub>2</sub>O<sub>5</sub>-WO<sub>3</sub>/TiO<sub>2</sub> catalyst for low temperature SCR of NO with NH<sub>3</sub>. *J. Solid State Chem.* **2015**, *221*, 49–56. [CrossRef]
28. Zhang, S.; Zhong, Q. Promotional effect of WO<sub>3</sub> on O<sub>2</sub> over V<sub>2</sub>O<sub>5</sub>/TiO<sub>2</sub> catalyst for selective catalytic reduction of NO with NH<sub>3</sub>. *J. Mol. Catal. A Chem.* **2013**, *373*, 108–113. [CrossRef]
29. Madia, G.; Koebel, M.; Elsener, M.; Wokaun, A. Side Reactions in the Selective Catalytic Reduction of NO<sub>x</sub> with Various NO<sub>2</sub> Fractions. *Ind. Eng. Chem. Res.* **2002**, *41*, 4008–4015. [CrossRef]
30. Castellino, F.; Rasmussen, S.B.; Jansen, A.D.; Johnsson, J.E.; Fehrmann, R. Deactivation of vanadia-based commercial SCR catalysts by polyphosphoric acids. *Appl. Catal. B Environ.* **2008**, *83*, 110–122. [CrossRef]
31. Gao, Y.; Liu, Q.; Bian, L. Numerical Simulation and Optimization of Flow Field in the SCR Denitrification System on a 600 MW Capacity Units. *Energy Procedia* **2012**, *14*, 370–375. [CrossRef]
32. Guo, X.; Bartholomew, C.; Hecker, W.; Baxter, L. Effects of sulfate species on V<sub>2</sub>O<sub>5</sub>/TiO<sub>2</sub> SCR catalysts in coal and biomass-fired systems. *Appl. Catal. B Environ.* **2009**, *92*, 30–40. [CrossRef]
33. Soyer, S.; Uzun, A.; Senkan, S.; Onal, I. A quantum chemical study of nitric oxide reduction by ammonia (SCR reaction) on V<sub>2</sub>O<sub>5</sub> catalyst surface. *Catal. Today* **2006**, *118*, 268–278. [CrossRef]
34. Yao, H.; Chen, Y.; Wei, Y.; Zhao, Z.; Liu, Z.; Xu, C. A periodic DFT study of ammonia adsorption on the V<sub>2</sub>O<sub>5</sub> (001), V<sub>2</sub>O<sub>5</sub> (010) and V<sub>2</sub>O<sub>5</sub> (100) surfaces: Lewis versus Brønsted acid sites. *Surf. Sci.* **2012**, *606*, 1739–1748. [CrossRef]
35. Orsenigo, C.; Beretta, A.; Forzatti, P.; Svachula, J.; Tronconi, E.; Bregani, F.; Baldacci, A. Theoretical and experimental study of the interaction between NO<sub>x</sub> reduction and SO<sub>2</sub> oxidation over DeNO<sub>x</sub>-SCR catalysts. *Catal. Today* **1996**, *27*, 15–21. [CrossRef]
36. Boudali, L.; Ghorbel, A.; Grange, P. Characterization and reactivity of WO<sub>3</sub>/V<sub>2</sub>O<sub>5</sub> supported on sulfated titanium pillared clay catalysts for the SCR-NO reaction. *C. R. Chim.* **2009**, *12*, 779–786. [CrossRef]
37. Querel, C.; Bonfils, A.; Grondin, O.; Creff, Y. Control of a SCR system using a virtual NO<sub>x</sub> sensor. In Proceedings of the 7th IFAC Symposium on Advances in Automotive Control, Tokyo, Japan, 4–7 September 2013; pp. 9–14.
38. Bonfils, A.; Creff, Y.; Lepreux, O.; Petit, N. Closed-loop control of a SCR system using a NO<sub>x</sub> sensor cross-sensitive to NH<sub>3</sub>. In Proceedings of the 8th IFAC Symposium on Advanced Control of Chemical Processes, Singapore, 10–13 July 2012; pp. 738–743.
39. Kang, Z.; Qixin, Y.; Lizheng, Z.; YuKun, D.; Baomin, S.; Wang, T. Study of the performance, simplification and characteristics of SNCR de-NO<sub>x</sub> in large-scale cyclone separator. *Appl. Therm. Eng.* **2017**, *123*, 635–645. [CrossRef]
40. Daood, S.S.; Javed, M.T.; Gibbs, B.M.; Nimmo, W. NO<sub>x</sub> control in coal combustion by combining biomass co-firing, oxygen enrichment and SNCR. *Fuel* **2013**, *105*, 283–292. [CrossRef]
41. Li, S.; Huang, W.; Xu, H.; Chen, T.; Ke, Y.; Qu, Z.; Yan, N. Alkali-induced deactivation mechanism of V<sub>2</sub>O<sub>5</sub>-WO<sub>3</sub>/TiO<sub>2</sub> catalyst during selective catalytic reduction of NO by NH<sub>3</sub> in aluminum hydrate calcining flue gas. *Appl. Catal. B Environ.* **2020**, *270*, 118872. [CrossRef]
42. Song, L.; Chao, J.; Fang, Y.; He, H.; Li, J.; Qiu, W.; Zhang, G. Promotion of ceria for decomposition of ammonia bisulfate over V<sub>2</sub>O<sub>5</sub>-MoO<sub>3</sub>/TiO<sub>2</sub> catalyst for selective catalytic reduction. *Chem. Eng. J.* **2016**, *303*, 275–281. [CrossRef]
43. Putluru, S.; Schill, L.; Godiksen, A.; Poreddy, R.; Mossin, S.; Jensen, A.; Fehrmann, R. Promoted V<sub>2</sub>O<sub>5</sub>/TiO<sub>2</sub> catalysts for selective catalytic reduction of NO with NH<sub>3</sub> at low temperatures. *Appl. Catal. B Environ.* **2016**, *183*, 282–290. [CrossRef]
44. Koebel, M.; Madia, G.; Raimondi, F.; Wokaun, A. Enhanced Reoxidation of Vanadia by NO<sub>2</sub> in the Fast SCR Reaction. *J. Catal.* **2002**, *209*, 159–165. [CrossRef]
45. U.S. Environmental Protection Agency, “Nitrogen Oxides (NO<sub>x</sub>), Why and How They Are Controlled,” 1999. [Online]. Available online: <http://www.epa.gov/ttn/catc>. (accessed on 5 September 2020).
46. Salazar, M.; Hoffmann, S.; Singer, V.; Becker, R.; Grunert, W. Hybrid catalysts for the selective catalytic reduction (SCR) of NO by NH<sub>3</sub>. On the role of fast SCR in the reaction network. *Appl. Catal. B Environ.* **2016**, *199*, 433–438. [CrossRef]



47. Li, Q.; Hou, X.; Yang, H.; Ma, Z.; Zheng, J.; Liu, F.; Zhang, X.; Yuan, Z. Promotional effect of CeO<sub>x</sub> for NO reduction over V<sub>2</sub>O<sub>5</sub>/TiO<sub>2</sub>-carbon nanotube composites. *J. Mol. Catal. A: Chem.* **2012**, *356*, 121–127. [CrossRef]
48. Li, F.; Shen, B.; Tian, L.; Li, G.; He, C. Enhancement of SCR activity and mechanical stability on cordierite supported V<sub>2</sub>O<sub>5</sub>-WO<sub>3</sub>/TiO<sub>2</sub> catalyst by substrate acid pretreatment and addition of silica. *Powder Technol.* **2016**, *297*, 384–391. [CrossRef]
49. Chen, M.; Zhao, M.; Tang, F.; Ruan, L.; Yang, H.; Li, N. Effect of Ce doping into V<sub>2</sub>O<sub>5</sub>-WO<sub>3</sub>/TiO<sub>2</sub> catalysts on the selective catalytic reduction of NO<sub>x</sub> by NH<sub>3</sub>. *J. Rare Earths* **2017**, *35*, 1206–1215. [CrossRef]
50. Shen, M.; Xu, L.; Wang, J.; Li, C.; Wang, W.; Wang, J.; Zhai, Y. Effect of synthesis methods on activity of V<sub>2</sub>O<sub>5</sub>/CeO<sub>2</sub>/WO<sub>3</sub>-TiO<sub>2</sub> catalyst for selective catalytic reduction of NO<sub>x</sub> with NH<sub>3</sub>. *J. Rare Earths* **2016**, *34*, 259–267. [CrossRef]
51. Shwan, S.; Partridge, W.; Choi, J.; Olsson, L. Kinetic modeling of NO<sub>x</sub> storage and reduction using spatially resolved MS measurements. *Appl. Catal. B Environ.* **2014**, *147*, 1028–1041. [CrossRef]
52. Dolanc, G.; Strmcnik, S.; Petrovic, J. NO<sub>x</sub> selective catalytic reduction control based on simple models. *J. Process Control* **2001**, *11*, 35–51. [CrossRef]
53. Chen, C.; Cao, Y.; Liu, S.; Chen, J.; Jia, W. SCR catalyst doped with copper for synergistic removal of slip ammonia and elemental mercury. *Fuel Process. Technol.* **2018**, *181*, 268–278. [CrossRef]
54. Krishnan, A.T.; Boehman, A.L. Selective catalytic reduction of nitric oxide with ammonia at low temperatures. *Appl. Catal. B Environ.* **1998**, *18*, 189–198. [CrossRef]
55. Zheng, C.; Wang, Y.; Liu, Y.; Yang, Z.; Qu, R.; Ye, D.; Liang, C.; Liu, S.; Gao, X. Formation, transformation, measurement, and control of SO<sub>3</sub> in coal-fired power plants. *Fuel* **2019**, *241*, 327–346. [CrossRef]
56. Zhao, Y.; Yang, W.; Zhou, J.; Wang, Z.; Liu, J.; Cen, K. Experimental study on ammonia adsorption by coal ashes. *J. Fuel Chem. Technol.* **2015**, *43*, 266–272. [CrossRef]
57. Zyrkowski, M.; Neto, R.C.; Santos, L.; Witkowski, K. Characterization of fly-ash cenospheres from coal-fired power plant unit. *Fuel* **2016**, *174*, 49–53. [CrossRef]
58. EPRI. *State-of-Knowledge of Fate, Removal, and Impact of Ammonia in Ash*; Report no. 1004700; Electric Power Research Institute: Palo Alto, CA, USA, 2002.
59. EPRI. *Investigation of Ammonia Adsorption on Fly Ash and Potential Impacts of Ammoniated Ash*; Report no. TR-113777; Electric Power Research Institute: Palo Alto, CA, USA, 1999.
60. Wang, X.; Zhang, J.; Wang, Z.; Wang, Y.; Vujanovic, M.; Li, P.; Tan, H. Experimental and kinetics study on SO<sub>3</sub> catalytic formation by Fe<sub>2</sub>O<sub>3</sub> in oxy-combustion. *J. Environ. Manag.* **2019**, *236*, 420–427. [CrossRef]
61. Zyrkowski, M.; Zymelka, P. Modelling of flexible boiler operation in coal fired power plant. *IOP Conf. Ser. Earth Environ. Sci.* **2019**, *214*, 012074. [CrossRef]
62. Sporn, R.; Maier, J.; Scheffknecht, G. Sulphur Oxide Emissions from Dust-Fired Oxy-Fuel Combustion of Coal. *Energy Procedia* **2013**, *37*, 1435–1447. [CrossRef]
63. Dunn, J.P.; Koppula, P.R.; Stenger, H.G.; Wachs, I.E. Oxidation of sulfur dioxide to sulfur trioxide over supported vanadia catalysts. *Appl. Catal. B Environ.* **1998**, *19*, 103–117. [CrossRef]
64. EPRI. *Modeling of SO<sub>3</sub> Formation Process in Coal-Fired Boilers*; Report no. 1012689; Electric Power Research Institute: Palo Alto, CA, USA, 2007.
65. Charles, A. Lockert, Breen Energy Solution., “Dynamic Control of SCR Minimum Operating Temperature,” [Online]. Available online: <https://breenes.com/>. (accessed on 6 September 2020).
66. Lu, J.; Zhou, Z.; Zhang, H.; Yang, Z. Influenced factors study and evaluation for SO<sub>2</sub>/SO<sub>3</sub> conversion rate in SCR process. *Fuel* **2019**, *245*, 528–533. [CrossRef]
67. Breen Energy Solutions, “Comprehensive acid gas management,” [Online]. Available online: [http://breenes.com/wp-content/uploads/2017/04/Comprehensive\\_Condensable\\_Management\\_Program-RevA.pdf](http://breenes.com/wp-content/uploads/2017/04/Comprehensive_Condensable_Management_Program-RevA.pdf). (accessed on 29 July 2019).
68. Forzatti, P.; Nova, I.; Beretta, A. Catalytic properties in deNO<sub>x</sub> and SO<sub>2</sub>–SO<sub>3</sub> reactions. *Catal. Today* **2000**, *56*, 431–441. [CrossRef]
69. EPRI. *Formation of N<sub>2</sub>O and NO<sub>2</sub> Across Conventional DeNO<sub>x</sub> SCR Catalysts*; Report no. 1019614; Electric Power Research Institute: Palo Alto, CA, USA, 2009.
70. Qing, M.; Su, S.; Wang, L.; Liu, L.; Sun, Z.; Mostafa, M.; Xu, K.; Hu, S.; Wang, Y.; Xiang, J. Effects of H<sub>2</sub>O and CO<sub>2</sub> on the catalytic oxidation property of V/W/Ti catalysts for SO<sub>3</sub> generation. *Fuel* **2019**, *237*, 545–554. [CrossRef]



71. Li, Y.; Zhu, Q.; Yi, Q.; Zuo, W.; Feng, Y.; Chen, S.; Dong, Y. Experimental method for observing the fate of  $\text{SO}_3/\text{H}_2\text{SO}_4$  in a temperature decreasing flue gas flow: Creation of state diagram. *Fuel* **2019**, *249*, 449–456. [\[CrossRef\]](#)
72. Li, Z.; Sun, F.; Shi, Y.; Li, F.; Ma, L. Experimental study and mechanism analysis on low temperature corrosion of coal fired boiler heating surface. *Appl. Therm. Eng.* **2015**, *80*, 355–361. [\[CrossRef\]](#)
73. Qi, G.; Yang, R.T. Performance and kinetics study for low-temperature SCR of NO with  $\text{NH}_3$  over  $\text{MnOx-CeO}_2$  catalyst. *J. Catal.* **2003**, *217*, 434–441. [\[CrossRef\]](#)
74. Hammershoi, P.S.; Vennestrom, P.N.; Falsig, H.; Jansen, A.D.; Janssens, T.V. Importance of the Cu oxidation state for the  $\text{SO}_2$  poisoning of a Cu-SAPO-34 catalyst in the  $\text{NH}_3$ -SCR reaction. *Appl. Catal. B Environ.* **2018**, *236*, 377–383. [\[CrossRef\]](#)
75. Wang, X.; Du, X.; Zhang, L.; Chen, Y.; Yang, G.; Ran, J. Promotion of  $\text{NH}_4\text{HSO}_4$  decomposition in NO/ $\text{NO}_2$  contained atmosphere at low temperature over  $\text{V}_2\text{O}_5\text{-WO}_3/\text{TiO}_2$  catalyst for NO reduction. *Appl. Catal. A Gen.* **2018**, *559*, 112–121. [\[CrossRef\]](#)
76. Muzio, L.; Bogseth, S.; Himes, R.; Chien, Y.; Dunn-Rankin, D. Ammonium bisulfate formation and reduced load SCR operation. *Fuel* **2017**, *206*, 180–189. [\[CrossRef\]](#)
77. Menasha, J.; Dunn-Rankin, D.; Muzio, L.; Stallings, J. Ammonium bisulfate formation temperature in a bench-scale single-channel air preheater. *Fuel* **2011**, *90*, 2445–2453. [\[CrossRef\]](#)
78. Shi, Y.; Shu, H.; Zhang, Y.; Fan, H.; Zhang, Y.; Yang, L. Formation and decomposition of  $\text{NH}_4\text{HSO}_4$  during selective catalytic reduction of NO with  $\text{NH}_3$  over  $\text{V}_2\text{O}_5\text{-WO}_3/\text{TiO}_2$  catalysts. *Fuel Process. Technol.* **2016**, *150*, 141–147. [\[CrossRef\]](#)
79. Si, F.; Romero, C.; Yao, Z.; Schuster, E.; Xu, Z.; Morey, R.; Liebowitz, B. Optimization of coal-fired boiler SCRs based on modified support vector machine models and genetic algorithms. *Fuel* **2009**, *88*, 806–816. [\[CrossRef\]](#)
80. Ning, R.; Liu, X.; Zhu, T. Research progress of low-temperature SCR denitration catalysts. *Chin. J. Process Eng.* **2019**, *19*, 223–234.
81. Lee, S.M.; Kim, S.S.; Hong, S.C. Systematic mechanism study of the high temperature SCR of NOx by  $\text{NH}_3$  over a  $\text{W/TiO}_2$  catalyst. *Chem. Eng. Sci.* **2012**, *79*, 177–185.
82. Wang, F.; Shen, B.; Zhu, S.; Wang, Z. Promotion of Fe and Co doped Mn-Ce/ $\text{TiO}_2$  catalysts for low temperature  $\text{NH}_3$ -SCR with  $\text{SO}_2$  tolerance. *Fuel* **2019**, *249*, 54–60. [\[CrossRef\]](#)
83. Zang, S.; Zhang, G.; Qiu, W.; Song, L.; Zhang, R.; He, H. Resistance to  $\text{SO}_2$  poisoning of  $\text{V}_2\text{O}_5/\text{TiO}_2\text{-PILC}$  catalyst for the selective catalytic reduction of NO by  $\text{NH}_3$ . *Chin. J. Catal.* **2016**, *37*, 888–897. [\[CrossRef\]](#)
84. Xiao, H.; Chen, Y.; Qi, C.; Ru, Y. Effect of Na poisoning catalyst ( $\text{V}_2\text{O}_5\text{-WO}_3/\text{TiO}_2$ ) on denitration process and  $\text{SO}_3$  formation. *Appl. Surf. Sci.* **2018**, *433*, 341–348. [\[CrossRef\]](#)
85. Yan, Z.; Shi, X.; Yu, Y.; He, H. Alkali resistance promotion of Ce-doped vanadium-titanic-based  $\text{NH}_3$ -SCR catalysts. *J. Environ. Sci.* **2018**, *73*, 155–161. [\[CrossRef\]](#)
86. Tian, Y.; Yang, J.; Yang, C.; Lin, F.; Hu, G.; Kong, M.; Liu, Q. Comparative study of the poisoning effect of NaCl and  $\text{Na}_2\text{O}$  on selective catalytic reduction of NO with  $\text{NH}_3$  over  $\text{V}_2\text{O}_5\text{-WO}_3/\text{TiO}_2$  catalyst. *J. Energy Inst.* **2019**, *92*, 1045–1052. [\[CrossRef\]](#)
87. Kong, M.; Liu, Q.; Zhu, B.; Yang, J.; Li, L.; Zhou, Q.; Ren, S. Synergy of KCl and Hgel on selective catalytic reduction of NO with  $\text{NH}_3$  over  $\text{V}_2\text{O}_5\text{-WO}_3/\text{TiO}_2$  catalysts. *Chem. Eng. J.* **2015**, *264*, 815–823. [\[CrossRef\]](#)
88. Yu, W.; Wu, X.; Si, Z.; Weng, D. Influences of impregnation procedure on the SCR activity and alkali resistance of  $\text{V}_2\text{O}_5\text{-WO}_3/\text{TiO}_2$  catalyst. *Appl. Surf. Sci.* **2013**, *283*, 209–214. [\[CrossRef\]](#)
89. Li, X.; Liu, C.; Li, X.; Peng, Y.; Li, J. A neutral and coordination regeneration method of Ca-poisoned  $\text{V}_2\text{O}_5\text{-WO}_3/\text{TiO}_2$  SCR catalyst. *Catal. Commun.* **2017**, *100*, 112–116. [\[CrossRef\]](#)
90. Lisi, L.; Lasorella, G.; Malloggi, S.; Russo, G. Single and combined deactivating effect of alkali metals and HCl on commercial SCR catalysts. *Appl. Catal. B Environ.* **2004**, *50*, 251–258. [\[CrossRef\]](#)
91. Klimczak, M.; Kern, P.; Heinzelmann, T.; Lucas, M.; Claus, P. High-throughput study of the effects of inorganic additives and poisons on  $\text{NH}_3$ -SCR catalysts—Part I:  $\text{V}_2\text{O}_5\text{-WO}_3/\text{TiO}_2$  catalysts. *Appl. Catal. B Environ.* **2010**, *95*, 39–47. [\[CrossRef\]](#)
92. Tang, F.; Xu, B.; Shi, H.; Qiu, J.; Fan, Y. The poisoning effect of  $\text{Na}^+$  and  $\text{Ca}^{2+}$  ions doped on the  $\text{V}_2\text{O}_5/\text{TiO}_2$  catalysts for selective catalytic reduction of NO by  $\text{NH}_3$ . *Appl. Catal. B Environ.* **2010**, *94*, 71–76. [\[CrossRef\]](#)
93. Chen, L.; Li, J.; Ge, M. The poisoning effect of alkali metals doping over nano  $\text{V}_2\text{O}_5\text{-WO}_3/\text{TiO}_2$  catalysts on selective catalytic reduction of NOx by  $\text{NH}_3$ . *Chem. Eng. J.* **2011**, *170*, 531–537. [\[CrossRef\]](#)

94. Li, X.; Li, X.; Yang, R.T.; Mo, J.; Li, J.; Hao, J. The poisoning effect of calcium on  $V_2O_5$ - $WO_3$ / $TiO_2$  catalyst for the SCR reaction: Comparison of different forms of calcium. *Mol. Catal.* **2017**, *434*, 16–24. [\[CrossRef\]](#)
95. Zheng, Y.; Jensen, A.D.; Johnsson, J.E.; Thøgersen, J.R. Deactivation of  $V_2O_5$ - $WO_3$ - $TiO_2$  SCR catalyst at biomass fired power plants: Elucidation of mechanisms by lab- and pilot-scale experiments. *Appl. Catal. B Environ.* **2008**, *83*, 186–194. [\[CrossRef\]](#)
96. Dahlin, S.; Nilsson, M.; Backstrom, D.; Bergman, S.L.; Bengtsson, E.; Bernasek, S.L.; Pettersson, L.J. Multivariate analysis of the effect of biodiesel-derived contaminants on  $V_2O_5$ - $WO_3$ / $TiO_2$  SCR catalysts. *Appl. Catal. B Environ.* **2016**, *183*, 377–385. [\[CrossRef\]](#)
97. Liu, S.; Guo, R.; Sun, X.; Liu, J.; Pan, W.; Xin, Z.; Shi, X.; Wang, Z.; Liu, X.; Qin, H. The deactivation effect of Cl on  $V/TiO_2$  catalyst for  $NH_3$ -SCR process: A DRIFT study. *J. Energy Inst.* **2019**, *92*, 1610–1617. [\[CrossRef\]](#)
98. Andonova, S.; Vovk, E.; Sjöblom, J.; Ozensoy, E.; Olsson, L. Chemical deactivation by phosphorous under lean hydrothermal conditions over Cu/BEA  $NH_3$ -SCR catalysts. *Appl. Catal. B Environ.* **2014**, *147*, 251–263. [\[CrossRef\]](#)
99. Wang, L.; Su, S.; Qing, M.; Dai, Z.; Sun, Z.; Liu, L.; Wang, Y.; Hu, S.; Xu, K.; Xiang, J. Melting solidification and leaching behavior of V/As during co-combustion of the spent SCR catalyst with coal. *Fuel* **2019**, *252*, 164–171. [\[CrossRef\]](#)
100. Peng, Y.; Si, W.; Li, X.; Luo, J.; Li, J.; Crittenden, J.; Hao, J. Comparison of  $MoO_3$  and  $WO_3$  on arsenic poisoning  $V_2O_5$ / $TiO_2$  catalyst: DRIFTS and DFT study. *Appl. Catal. B Environ.* **2016**, *181*, 692–698. [\[CrossRef\]](#)
101. Xu, Y.; Zhang, Y.; Liu, F.; Shi, W.; Yuan, J. CFD analysis on the catalyst layer breakage failure of an SCR-DeNOx system for a 350 MW coal-fired power plant. *Comput. Chem. Eng.* **2014**, *69*, 119–127. [\[CrossRef\]](#)
102. Nova, I.; Ciardelli, C.; Tronconi, E.; Chatterjee, D.; Bandl-Konrad, B.  $NH_3$ -NO/ $NO_2$  chemistry over V-based catalysts and its role in the mechanism of the Fast SCR reaction. *Catal. Today* **2006**, *114*, 3–12. [\[CrossRef\]](#)
103. Lang, E.; Drtina, P. Numerical simulation of the fluid flow and the mixing process in a static mixer. *Int. J. Heat Mass Transf.* **1995**, *38*, 2239–2250. [\[CrossRef\]](#)
104. Xu, Y.; Zhang, Y.; Wang, J.; Yuan, J. Application of CFD in the optimal design of a SCR-DeNOx system for a 3000 MW coal-fired power plant. *Comput. Chem. Eng.* **2013**, *49*, 50–60. [\[CrossRef\]](#)
105. Khatun, N.; Tiwari, S.; Lal, J.; Tseng, C.; Liu, S.W.; Biring, S.; Sen, S. Stabilization of anatase phase by uncompensated Ga-V co-doping in  $TiO_2$ : A structural phase transition, grain growth and optical property study. *Ceram. Int.* **2018**, *44*, 22445–22455. [\[CrossRef\]](#)
106. Byrne, C.; Moran, L.; Hermosilla, D.; Merayo, N.; Blanco, A.; Rhatigan, S.; Hinder, S.; Ganguly, P.; Nolan, M.; Pillai, S. Effect of Cu doping on the anatase-to-rutile phase transition in  $TiO_2$  photocatalysts: Theory and experiments. *Appl. Catal. B Environ.* **2019**, *246*, 266–276. [\[CrossRef\]](#)
107. Hanaor, D.; Sorrell, C. Review of the anatase to rutile phase transformation. *J. Mater. Sci.* **2011**, *46*, 855–874. [\[CrossRef\]](#)
108. Liu, R.; Li, H.; Duan, L.; Shen, H.; Zhang, Q.; Zhao, X. Influences of annealing atmosphere on phase transition temperature, optical properties and photocatalytic activities of  $TiO_2$  phase-junction microspheres. *J. Alloys Compd.* **2019**, *789*, 1015–1021. [\[CrossRef\]](#)
109. Dauksta, E.; Medvids, A.; Onufrijevs, P.; Shimomura, M.; Fakuda, Y.; Murakami, K. Laser-induced crystalline phase transition from rutile to anatase of niobium doped  $TiO_2$ . *Curr. Appl. Phys.* **2019**, *19*, 351–355. [\[CrossRef\]](#)
110. Du, X.; Wu, Y.; Kou, Y.; Mu, J.; Yang, Z.; Hu, X.; Teng, F. Amorphous carbon inhibited  $TiO_2$  phase transition in aqueous solution and its application in photocatalytic degradation of organic dye. *J. Alloys Compd.* **2019**, *810*, 151917. [\[CrossRef\]](#)
111. Chen, H.; Xia, Y.; Fang, R.; Huang, H.; Gan, Y.; Liang, C.; Zhang, J.; Zhang, W.; Liu, X. The effects of tungsten and hydrothermal aging in promoting  $NH_3$ -SCR activity on  $V_2O_5$ / $WO_3$ - $TiO_2$  catalysts. *Appl. Surf. Sci.* **2018**, *459*, 639–646. [\[CrossRef\]](#)
112. Zhao, K.; Han, W.; Tang, Z.; Zhang, G.; Lu, J.; Lu, G.; Zhen, X. Investigation of coating technology and catalytic performance over monolithic  $V_2O_5$ - $WO_3$ / $TiO_2$  catalyst for selective catalytic reduction of  $NO_x$  with  $NH_3$ . *Colloids Surf. A Physicochem. Eng. Asp.* **2016**, *503*, 53–60. [\[CrossRef\]](#)
113. Khatun, N.; Anita; Rajput, P.; Bhattacharya, D.; Jha, S.; Biring, S.; Sen, S. Anatase to rutile phase transition promoted by vanadium substitution in  $TiO_2$ : A structural, vibrational and optoelectronic study. *Ceram. Int.* **2017**, *43*, 14128–14134.
114. Liu, X.; Wu, X.; Xu, T.; Weng, D.; Si, Z.; Ran, R. Effects of silica additive on the  $NH_3$ -SCR activity and thermal stability of a  $V_2O_5$ / $WO_3$ - $TiO_2$  catalyst. *Chin. J. Catal.* **2016**, *37*, 1340–1346. [\[CrossRef\]](#)

115. Sun, C.; Dong, L.; Yu, W.; Liu, L.; Li, H.; Gao, F.; Dong, L.; Chen, Y. Promotion effect of tungsten oxide on SCR of NO with NH<sub>3</sub> for the V<sub>2</sub>O<sub>5</sub>-WO<sub>3</sub>/Ti<sub>0.5</sub>Sn<sub>0.5</sub>O<sub>2</sub> catalyst: Experiments combined with DFT calculations. *J. Mol. Catal. A Chem.* **2011**, *346*, 29–38. [[CrossRef](#)]
116. Marberger, A.; Elsener, M.; Nuguid, M.; Ferri, D.; Krocher, O. Thermal activation and aging of a V<sub>2</sub>O<sub>5</sub>/WO<sub>3</sub>-TiO<sub>2</sub> catalyst for the selective catalytic reduction of NO with NH<sub>3</sub>. *Appl. Catal. A General* **2019**, *573*, 64–72. [[CrossRef](#)]
117. Nova, I.; dall'Acqua, L.; Lietti, L.; Giamello, E.; Forzatti, P. Study of thermal deactivation of a de-NO<sub>x</sub> commercial catalyst. *Appl. Catal. B Environ.* **2001**, *35*, 31–42. [[CrossRef](#)]
118. Ma, Z.; Deng, J.; Li, Z.; Li, Q.; Zhao, P.; Wang, L.; Sun, Y.; Zheng, H.; Pan, L.; Zhao, S.; et al. Characteristics of NO<sub>x</sub> emission from Chinese coal-fired power plants equipped with new technologies. *Atmos. Environ.* **2016**, *131*, 164–170. [[CrossRef](#)]
119. Tomeczek, J. *Coal Combustion*; Krieger Publishing Company: Malabar, FL, USA, 1994.
120. Bujalski, M.; Zyrkowski, M.; Nabaglo, D.; Szczepanek, K. The algorithm of steam soot blowers operation based on the monitoring of fouling factors of heating surfaces of a coal-fired boiler under operating conditions. *E3S Web Conf.* **2019**, *82*, 01001. [[CrossRef](#)]

**Publisher's Note:** MDPI stays neutral with regard to jurisdictional claims in published maps and institutional affiliations.



© 2020 by the authors. Licensee MDPI, Basel, Switzerland. This article is an open access article distributed under the terms and conditions of the Creative Commons Attribution (CC BY) license (<http://creativecommons.org/licenses/by/4.0/>).